# Direct measurement of the dielectric frame rotation of monoclinic crystals as a function of the wavelength

Christian Traum, Patricia Loren-Inacio, Corinne Felix, Patricia Segonds, Alexandra Pena, Jérome Debray, Benoit Boulanger, Yannick Petit, Daniel Rytz, G. Montemezzani, et al.

# Direct measurement of the dielectric frame rotation of monoclinic crystals as a function of the wavelength

**C. Traum,[1,2] P. L. Inácio, [1,2] C. Félix,[1,2] P. Segonds,[1,2*] A. Peña,[1,2] J. Debray,[1,2] B. Boulanger,[1,2] Y. Petit,[3,4] D. Rytz,[5] G. Montemezzani,[6] P. Goldner,[7] and A. Ferrier[7]**

[1]*Univ. Grenoble Alpes, Inst NEEL, F-38042 Grenoble, France*
[2]*CNRS, Inst NEEL, F-38042 Grenoble, France*
[3]*Univ. Bordeaux, ICMCB, UPR 9048, F-33600 Pessac, France*
[4]*CNRS, ICMCB, UPR 9048, F-33608 Pessac, France*
[5]*FEE GmbH, Struthstr. 2, 55743 Idar-Oberstein, Germany*
[6]*Laboratoire Matériaux Optiques, Photonique et Systèmes (LMOPS, EA 4423), Université de Lorraine and Supélec, F-57070 Metz, France*
[7]*LCMCP CNRS UMR 7574, ENSCP - Chimie Paristech, rue P. et M. Curie, F-75005 Paris, France*
**patricia.segonds@neel.cnrs.fr*

**Abstract:** We report a method based on Malus' law to directly measure the dielectric frame orientation of monoclinic crystals with an accuracy of 0.3°. This technique was validated by the study of $Nd^{3+}$:$YCa_4O(BO_3)_3$, $Sn_2P_2S_6$, $BiB_3O_6$ and $Eu^{3+}$:$Y_2SiO_5$.



**OCIS codes:** (260.1180) Crystal optics; (260.5430) Polarization; (260.2030) Dispersion.

**References and links**

1. J. F. Nye, *Physical Properties of Crystals* (Clarendon Press, 1957).
2. B. Boulanger and J. Zyss, "Nonlinear optical properties," International Tables of Crystallography, **D**, 178–219 (2006).
3. D. Haertle, A. Guarino, J. Hajfler, G. Montemezzani, and P. Günter, "Refractive indices of $Sn_2P_2S_6$ at visible and infrared wavelengths," Opt. Express **13**(6), 2047–2057 (2005).
4. H. Hellwig, J. Liebertz, and L. Bohaty, "Linear optical properties of the monoclinic bismuth borate $BiB_3O_6$," J. Appl. Phys. **88**(1), 240–244 (2000).
5. P. Segonds, B. Boulanger, B. Ménaert, J. Zaccaro, J. P. Salvestrini, M. D. Fontana, R. Moncorgé, F. Porée, G. Gadret, J. Mangin, A. Brenier, G. Boulon, G. Aka, and D. Pelenc, "Optical characterizations of $YCa_4O(BO_3)_3$ and Nd: $YCa_4O(BO_3)_3$ crystals," Opt. Mater. **29**(8), 975–982 (2007).
6. A. N. Winchell, *Elements of Optical Mineralogy, Part I Principles and Methods*, 5th edition (John Wiley & Sons Inc., 1965).
7. E. Hecht, *Optics*, 3rd Edition (Addison Wesley, 1994).
8. C. Li, C. Wyon, and R. Moncorgé, "Spectroscopic properties and fluorescence dynamics of $Er^{3+}$ and $Yb^{3+}$ in $Y_2SiO_5$," IEEE J. Quantum Electron. **28**(4), 1209–1221 (1992).
9. Y. Petit, S. Joly, P. Segonds, and B. Boulanger, "Recent advances in monoclinic crystals," Laser Photonics Rev. **7**(6), 920–937 (2013).

## 1. Introduction

Monoclinic crystals are biaxial crystals, so that they have three different principal refractive indices in the orthonormal dielectric frame (*x, y, z*) [1]. It is also well known that in monoclinic crystals the orientation of the dielectric frame does not correspond to that of the crystallographic frame (*a, b, c*) since it is not orthonormal [2]. There are three monoclinic point groups: *m*, *2* and *2/m* where *2* stand for a two-fold axis and *m* for the mirror plane. One crystallographic axis is called the "special axis" [2]: it is parallel to the *2*-fold axis for point groups *2* and *2/m*, and perpendicular to the mirror plane *m* for point group *m* and *2/m*. The special axis is perpendicular to the two other crystallographic axes, and the angle between these two axes, labeled β, is larger than 90°. According to the classical convention, *b* is taken as the special axis and from reported experimental results, it can coincide with the axis *x*, *y* or *z* of the dielectric frame [3–5].

#199811 - $15.00 USD Received 18 Oct 2013; revised 22 Nov 2013; accepted 22 Nov 2013; published 10 Dec 2013

In the present paper we describe a method enabling the direct measurement of the angles between the dielectric and crystallographic frames as a function of the wavelength. It is based on polarization measurements using Malus' law recorded in the transparency range. The crystal under study is cut as a slab with two polished faces perpendicular to the special axis of the crystallographic frame. Our method has the advantage to use a simple crystal shape and to provide a direct measurement of the dielectric frame orientation without any intermediate measurements and calculations as in [3–5]. We considered three monoclinic crystals for validating this method: $Nd^{3+}$:$YCa_4O(BO_3)_3$ and $Sn_2P_2S_6$, that belong to the point group *m*, and $BiB_3O_6$ (point group *2*). We also report the first measurement of $Eu^{3+}$:$Y_2SiO_5$ (point group *2/m*).

## 2. Description of the method

Due to the diversity of reported orientations between the dielectric and crystallographic axes, we chose in the present paper to label the three axes of the dielectric frame $d_1$, $d_2$ and $d_3$, each of them being the *x*-, *y*- or *z*-axis [3–5], and $d_1$ coincides with the special axis *b*. Then the four other axes, *i.e. a, c,* $d_2$ and $d_3$ are located in the plane that is perpendicular to the special axis *b* = $d_1$. We describe the relative orientation between the crystallographic and dielectric frames in this plane by using the angle $\varphi=(a, d_3)$, where $d_3$ is the nearest dielectric axis from the crystallographic *a*-axis. Then two configurations are possible corresponding to $d_3$-axis as shown in Fig. 1(a). The angle between the crystallographic and the dielectric frames is $(c,d_2)=\varphi-\beta+90°$ or $(c,d_2)=\varphi+\beta-90°$.

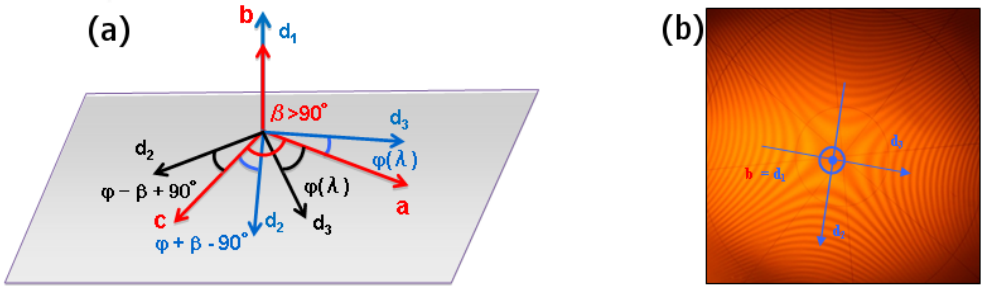


Fig. 1. a) Two possible configurations between the crystallographic frame (*a, b, c*) and the dielectric frame ($d_1$, $d_2$, $d_3$) in a monoclinic crystal. *b*-axis is the special axis. λ is the wavelength of the propagating light. b) Conoscopy patterns at $\lambda_0$ = 0.633 µm through $BiB_3O_6$ slab with two polished faces perpendicular to *b*-axis where ($d_1$, $d_2$, $d_3$) is the dielectric frame.

By changing the wavelength, the temperature or any other dispersive parameters of the refractive index, the dielectric frame may rotate in the plane perpendicular to the special axis. On the other hand, the crystallographic frame orientation remains fixed because it is "attached" to the atoms [2]. It is then crucial to characterize this effect since any optical property depending on the refractive index is expressed in the dielectric frame.

Such a rotation has been previously reported at room temperature in the transparency range of two monoclinic crystals as a function of the wavelength: it is varying from 40° to 52° in $Sn_2P_2S_6$ (point group *m*) over the wavelength range between 0.5 µm and 2.2 µm [3], it is varying from 43° to 47° between 0.36 µm and 2.3 µm in $BiB_3O_6$ (point group *2*) [4]. However, it has been shown that the dielectric frame does not rotate in $Nd^{3+}$:$YCa_4O(BO_3)_3$ despite $Nd^{3+}$ electronic transitions in the studied wavelength range because the absorption is very weak [5]. In the case of $Sn_2P_2S_6$ and $BiB_3O_6$ the dispersion of the orientation angle $\varphi$ of the dielectric frame could be determined from the Sellmeier dispersion data obtained by measuring the deviation angles using two specifically oriented prisms [3, 4]. The study of $Nd^{3+}$:$YCa_4O(BO_3)_3$ was done using the internal conical refraction of light observed at the exit

#199811 - $15.00 USD Received 18 Oct 2013; revised 22 Nov 2013; accepted 22 Nov 2013; published 10 Dec 2013

of a millimeter size crystal sphere mounted on a goniometric head and placed on a rotating stage [5].

In the method presented here, a slab is cut and polished with two faces perpendicular to the *b*-axis and the orientation of *a*- and *c*- axes are identified by X-raying the crystal in a backscattered Laue geometry, with a precision of 0.25°. Then we performed transmission conoscopy by viewing the sample along its *b*-axis [6]. We used a microscope coupled to a He-Ne laser emitting at $\lambda_0$ = 0.633 µm. This leads to interference patterns whose axes of symmetry correspond to the three axes of the dielectric frame that are shown in Fig. 1(b) corresponding to the example of $BiB_3O_6$. Following the Laue Diagram and the definitions in Fig. 1(a), the symmetry axes of the pattern correspond to the dielectric axes $d_1$, $d_2$ and $d_3$ [6]. The accuracy of the dielectric axes orientation is less than 1°. From the combination of the results obtained with X-rays diffraction and conoscopy at $\lambda_0$ = 0.633 µm, it is possible to determine the relative orientation of the crystallographic and dielectric frames, i.e. $\varphi(\lambda_0)$. We did not try to assign $(d_1, d_2, d_3)$ to $(x, y, z)$. Indeed, the present work focuses only on the magnitude of $\varphi$ as a function of the wavelength $\lambda$.

The crystal slab is then inserted between two crossed polarizers: we used two Glan-Taylor prisms with a $10^{-5}$ extinction rate. A tunable laser beam propagates at normal incidence along the *b*-axis through the two polished faces as shown in Fig. 2. Then by rotating the sample perpendicularly to the laser beam axis using a continuous piezoelectric motor, it was possible to measure the power transmitted by the exit polarizer, and thereby obtain the dielectric frame rotation, *i.e.* $\varphi$ as a function of the tunable wavelength $\lambda$.

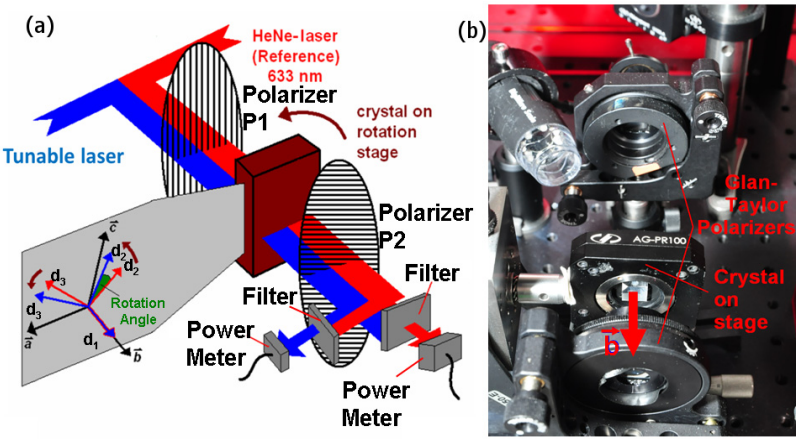


Fig. 2. Scheme (a) and picture (b) of the rotating monoclinic slab cut perpendicularly to the special axis, inserted between two crossed polarizers and irradiated by a tunable laser beam.

Our method uses the fact that monoclinic crystals are anisotropic media. Actually the two axes $d_2$ and $d_3$ of the dielectric frame correspond to the neutral lines in the conoscopy picture observed along $d_1$: they are associated with two linear polarization states that are perpendicular one to each other [7]. Consequently there is no transmitted light when $d_2$ or $d_3$ are collinear to the axis of the input or output polarizers. The transmitted power is maximal when they are at 45° from the polarizers axes, and for all other orientations, the transmitted power has an intermediate value. It is well known that the variation of the transmitted power through a crystal of length L inserted between two cross polarizers follows Malus' law when an anisotropic medium is rotating around an axis parallel to the direction of light propagation. By using the Jones matrices formalism [7], we calculated the transmitted power and got the following formula:

$$P_t(\lambda) = 2^{-1} P_0 \sin^2\left[2\varphi(\lambda)\right]\left\{1-\cos\left[2\pi\lambda^{-1}L(n_3(\lambda)-n_2(\lambda))\right]\right\}+P_r \qquad (1)$$

#199811 - $15.00 USD Received 18 Oct 2013; revised 22 Nov 2013; accepted 22 Nov 2013; published 10 Dec 2013

$P_0$ and $P_t$ are the input and output powers respectively, and $n_2$ and $n_3$ are the refractive indices eigenvalues associated with the propagation direction along the dielectric axis $d_1$. $P_r$ stands for the residual transmitted power due to an extinction rate of the polarizers deviating from $10^{-5}$.

The transmitted power $P_t$ was recorded synchronously with a piezoelectric motor that rotates the slab using a remote control as a function of time. We performed such a measurement using two lasers: a HeNe laser emitting at $\lambda_0$ = 0.633 µm, and a pulsed Optical Parametric Oscillator (OPO) from Continuum tunable between $\lambda$ = 0.4 µm and $\lambda$ = 2.4 µm. The repetition rate was 10 Hz, with a pulse length of 5 ns. The wavelength $\lambda$ was controlled using two spectrometers from Ocean Optics: $\lambda$ below 1.1 µm was measured with an accuracy of 0.1 nm, while it was 3 nm for longer wavelengths.

The transmitted OPO and He-Ne powers, $P_t(\lambda)$ and $P(\lambda_0)$ respectively, were simultaneously measured as shown in Fig. 2. We used two calibrated photodiode sensors PD300TP from OPHIR sensitive from 50 pW to 1 W over the wavelength range between 0.35 and 1.1 µm. By using also PD300IRG we were able to measure $P(\lambda_0)$ up to 1.5 microns. Consequently, $\varphi(\lambda)$ was recorded relatively to the value of $\varphi(\lambda_0)$. This double measurement is the strength of the method we propose. Firstly, it allows us to get rid of any non-linearity of the piezoelectric motor due to the sample or holder weight, and of a small precession during the rotation of the crystal. Secondly, it reveals directly the dielectric frame orientation of the studied crystal at the wavelength $\lambda$, corresponding to $\Delta\varphi(\lambda) = \varphi(\lambda) - \varphi(\lambda_0)$, as a direct phase-shift between the OPO and He-Ne Malus' laws. In the insert of Fig. 3, an example is provided of $P_t(\lambda$ = 0.7 µm) and $P_t(\lambda_0$ = 0.633 µm) recorded simultaneously for $BiB_3O_6$.

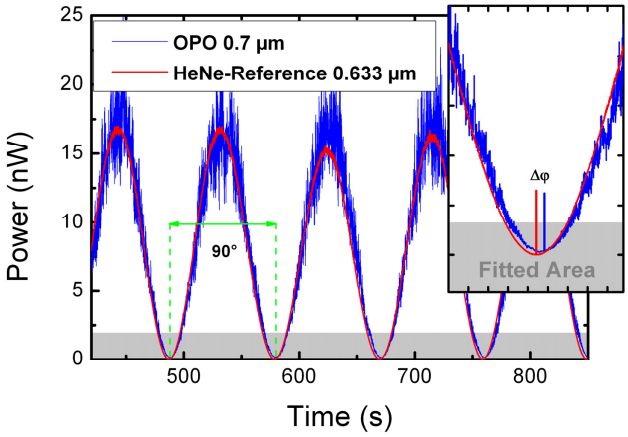


Fig. 3. Transmitted OPO (blue curve) and He-Ne (red curve) power as a function of time when the $BiB_3O_6$ slab is rotating continuously between crossed polarizers. In the insert, the phase shift resulting from the measurement at two different wavelengths, $\Delta\varphi(\lambda) = \varphi(\lambda) - \varphi(\lambda_0)$, is shown. Grey area is the selected part of consecutive minima interpolated with a second order polynomial to convert the time scale in seconds to angle in degrees.

The OPO and He-Ne transmitted powers and the phase-shift $\Delta\varphi(\lambda)$ were recorded as a function of time (see Fig. 3). The latter is converted to angles since the time period $T$ of Malus' law given by Eq. (1) is 90° [7]. In this case, $T$ is measured directly by considering for example the time elapsed between two consecutive minima of Malus' laws as shown in Fig. 3. However when we measured this interval, we found that $T$ varied for successive couples of consecutive minima. It was confirmed by the fact that the data cannot be fitted exactly by Eq. (1). By performing the interpolation of OPO and He-Ne Malus' law around minima with a second order polynomial, we were able to derive the standard deviation of their distribution of $T$ with the best accuracy. After converting time into angle, we derived $\varphi(\lambda)$ and $\varphi(\lambda_0)$ as the mean value of the distribution of T for OPO and He-Ne curves respectively. Their accuracy is

#199811 - $15.00 USD Received 18 Oct 2013; revised 22 Nov 2013; accepted 22 Nov 2013; published 10 Dec 2013

given by the standard deviations of T. With this method, the phase-shift $\Delta\varphi(\lambda) = \varphi(\lambda) - \varphi(\lambda_0)$ accuracy is ranged between 0.3° and 0.5°.

### 3. Validation of the method on $YCa_4O(BO_3)_3$, $Sn_2P_2S_6$ and $BiB_3O_6$

We considered three well known monoclinic crystals: $Nd^{3+}$:$YCa_4O(BO_3)_3$, $Sn_2P_2S_6$ and $BiB_3O_6$ [3–5]. The slabs dimensions were 8.28 x 8.14 x 4.08 $mm^3$, 11 x 2.77 x 7.5 $mm^3$ and 5.4 x 5.0 x 4.9 $mm^3$ respectively. They are depicted in Fig. 4, showing also our measurements of the relative orientation between (*a, b, c*) and ($d_1$, $d_2$, $d_3$) at $\lambda_0$, and the corresponding values of $\beta$ and $\varphi(\lambda_0)$ angles. Our data are in agreement with [3–5] that also give the correspondence between ($d_1$, $d_2$, $d_3$) and (*x, y, z*).

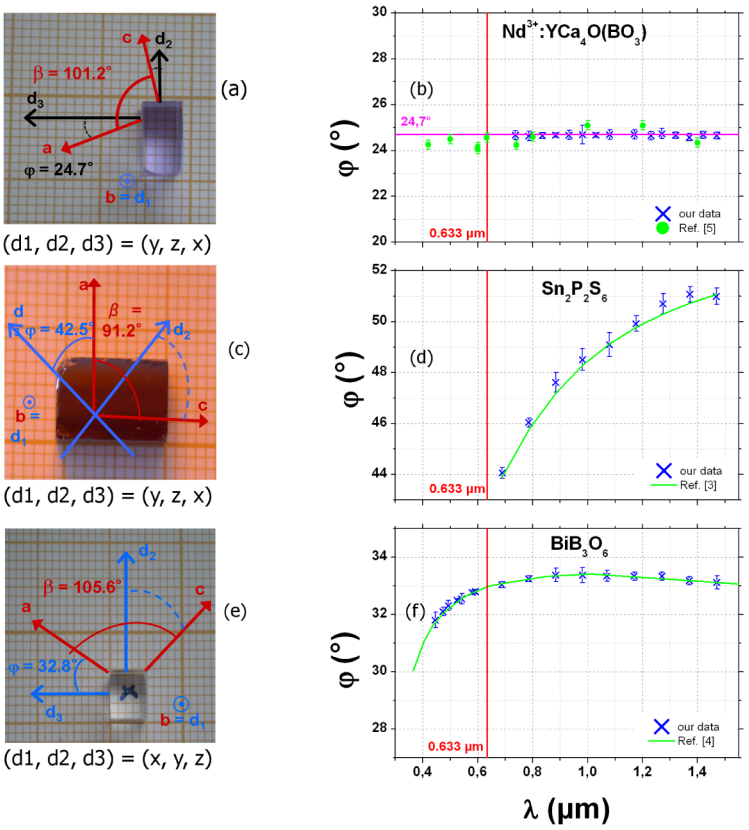


Fig. 4. Crystal orientations and magnitudes of $\varphi(\lambda)$ of $Nd^{3+}$:$YCa_4O(BO_3)_3$ (a) and (b), $Sn_2P_2S_6$ (c) and (d), $BiB_3O_6$ (e) and (f). The crystallographic axes *a*, *b*, *c* and β-angle are drawn on the crystal pictures, as well as the dielectric axes $d_1$, $d_2$, $d_3$ and $\varphi(\lambda_0)$ at $\lambda_0$ = 0.633 µm showing the two possible configurations of orientations between the crystallographic and dielectric frames.

$\Delta\varphi(\lambda)$ was recorded between 0.2 µm and 1.5 µm, and the corresponding values of $\varphi(\lambda)$ determined by subtracting $\varphi(\lambda_0)$. As shown in Fig. 4, the experimental values of $\varphi(\lambda)$ are in good agreement with the data given in [3–5], which validates our method.

### 4. First measurements in $Eu^{3+}$:$Y_2SiO_5$

The direct measurement of the dielectric frame rotation with our method being validated, we were able to study the rotation between the crystallographic and dielectric frames of any monoclinic crystal. Because of its recent interest in quantum information, we selected $Eu^{3+}$:$Y_2SiO_5$ which belongs to the point group *2/m* [8]. The slab dimensions were 14.1 x 5.18 x 15.2 $mm^3$, and $\beta$ = (a, c) = 102.7° as shown in Fig. 5. The orientation difference between the

#199811 - $15.00 USD Received 18 Oct 2013; revised 22 Nov 2013; accepted 22 Nov 2013; published 10 Dec 2013

crystallographic and dielectric frames leads to $\varphi(\lambda_0 = 0.633\ \mu m) = 23.4°$, which is in agreement with [8]. In Fig. 5 it is also shown the evolution of $\varphi(\lambda)$ from 0.4 µm to 1.5 µm. It puts in evidence for the first time to our knowledge a dielectric frame rotation of 3° in $Eu^{3+}:Y_2SiO_5$, which is twice that of $BiB_3O_6$ over this wavelength range. Such a rotation of the two polarization eigenmodes can be detrimental when the crystal is used as an optical memory and processor since it may reduce the associated value of the absorption cross-section [8, 9].

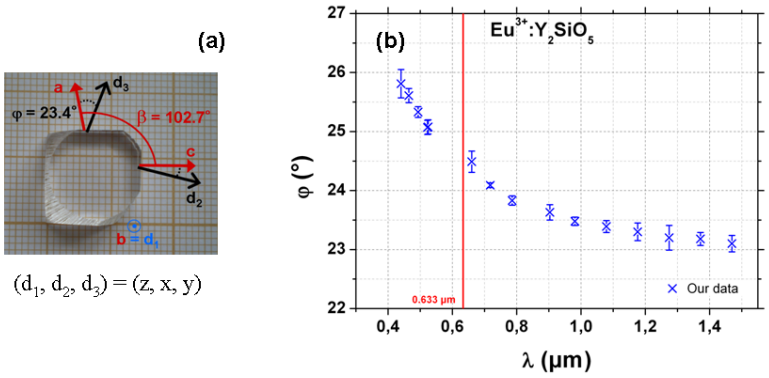


Fig. 5. $Eu^{3+}:Y_2SiO_5$: a) crystallographic axes *a*, *b*, *c,* dielectric axes $d_1$, $d_2$, $d_3$, and $\beta$-angle drawn on the crystal picture, b) magnitude of the angle $\varphi$ as a function of the wavelength $\lambda$ .

## 5. Conclusion

We conceived an experimental setup enabling the direct measurement of the dielectric frame orientation of monoclinic crystals as a function of wavelength between 0.4 and 2.4 µm. It has the advantage to use slabs cut perpendicular to the easily identified special axis of the crystal. The orientation of the crystallographic frame is determined by X-raying the crystal in a backscattered Laue geometry. The oriented slab being inserted between two crossed polarizers and rotating continuously, the dielectric frame orientation is determined from recording the transmitted power of an OPO and a He-Ne laser as a function of time simultaneously. We validated our method over the wavelength range between 0.4 and 1.5 µm by studying the three well-known monoclinic crystals $Nd^{3+}:YCa_4O(BO_3)_3$, $Sn_2P_2S_6$ and $BiB_3O_6$. We also studied $Eu^{3+}:Y_2SiO_5$ and we report a dielectric frame rotation of 3° in this range. Future work will analyse the behaviour of this rotation as a function of temperature.


## Acknowledgment

The Mission Interdisciplinaire (MI) of Centre National de la Recherche Scientifique (CNRS), Conselho Nacional de Desenvolvimento Científico e Tecnológico (CNPq) for their financial supports, A. A. Grabar for the $Sn_2P_2S_6$ sample used in this work.


#199811 - $15.00 USD Received 18 Oct 2013; revised 22 Nov 2013; accepted 22 Nov 2013; published 10 Dec 2013